PRECISE TEMPERATURE CONTROL OF INERTIAL SENSORS USING CONVENTIONAL CONTROLLERS, HEATERS AND PELTIER ELEMENTS

VALERI V. VLASSOV, PAULO GIÁCOMO MILANI

Instituto Nacional de Pesquisas Espaciais – INPE
Space Mechanic and Control Division - DMC
Av. dos Astronautas 1758, Caixa Postal 515, 12227-010 São José dos Campos, SP
E-mails: vlassov@dem.inpe.br   milani@dem.inpe.br

Abstract— The reachable limits of precision of temperature control for a miniature rate gyro was evaluated through mathematical modeling. Two different environments were simulated: ground test laboratory conditions and Space flight conditions. The stability of temperature of the inertial sensor was used as a criterion for evaluation of the quality of the adopted thermal control. The analysis was performed as a parametric study with variation of such design parameters as thermal conductance of the mechanical interface, effectiveness of radiator, type of Peltier element etc. The influence of the parameters of control was also evaluated: a sensitivity analysis was performed for variations of PID gains, maximal power and on-off dead-band. Results of simulations are presented; the best thermal stability achieved was ±0.5 ^{0}C for ground conditions and ±1.3 ^{0}C for Space conditions.

Keywords— inertial sensor, Peltier element, thermo - electric cooler, thermal control.

1 Introduction

Inertial sensors (IS) are those that provide their outputs relative to an inertial reference frame, i.e., a reference that is considered ideal and that would be fixed in relation to the stars.

Inertial sensors enable the measurement of displacements in space in a very convenient form, even interplanetary travel, inside or outside of the influence of the gravitational field of a planet, even though they may have intrinsic errors that are influenced by different environmental factors.

The two basic sensors of interest for navigation of ships, airplanes, rockets and satellites are the gyroscopes and the accelerometers, both to be considered in this work.

Independently of the technology used to build it and depending on the precision desired for the sensor, it is very important that the environmental conditions are held constant so that they have the least influence on the behavior of the sensor. This way it is very common that the use of this kind of sensors may require the consideration of many factors that influence their performance and the means to block or to compensate that influence.

Electromagnetic fields, as an example, may influence inadequately the behavior of sensors that have their principle of operation based on those fields and therefore they may need to be shielded from both the electrical or magnetic fields. That may be the case of some gyroscopes like the DTG (Dry tuned Gyro). Its outside body is built from a magnetic conducting material.

Vibrations can be decreased with the use of the sensor with a special support, a kind of a suspension that works as a filter and eliminates most of the vibrations that may be induced by unwanted accelerations.

The environment air may cause corrosion and bring acoustic noise but on the other hand it may enable the dissipation of heat by means of conduction and convection.

The dynamics of the vehicle also affects the performance of the sensor that it carries, imposing different workloads with different power dissipation conditions. The outside temperature also influences the sensors, driving less or more heat that the sensor produces, influencing its operating point.

Gyroscopes and other inertial sensors, those made by traditional mechanical means and also the ones made by MEMS techniques are very sensible to the mechanical environment and particularly to temperature variation.

Normally inertial sensors undergo a number of thermal tests and based on the output results it is possible to obtain input/output curves and the polynomial indication of their behavior.

The thermal environment has many implications on the performance of an electromechanical device. In considering only the influence of the generated heat caused by the torquer, Lacchini and Mansour mention the following:

1. a shift of the demagnetization curves to the right and a decrease of the remanence of the permanent magnet (B_a). To maintain the same value of the reaction torque or the dynamic range, one should use a higher value for the current of the torquer, what implies in greater losses due to I^2R,
2. an increase in the resistivity of the conductor which causes a futher increase in the I^2R term,
3. an increase in the heat transfer coefficient, which brings changes in the thermal balance of the coil.

Other sensors that employ the same working principle in torquers, like accelerometers, they have the same problems of cause and effect.

To be able to live with the problems as above described in the fabrication of systems of high precision sensors, it is common practice the use of techniques of compensation of the corresponding output data.

Generally these compensations occur in the form of polynomials where there are proportionality factors for each of the error parameters of the sensor. These polynomials are, actually, approximations determined by performance of smaller or greater precision tests indicating how much and in which way a determined parameter of a sensor varies. A typical example as presented bellow, obtained from Dorobantu (1999) for the case of an accelerometer.

$$u = D + H + k_0 + k_{01}t + k_{01}t_2 + k_1 f_1 +$$
$$k_2 f_{12} + k_3 f_{13} + k_{12no} f_2 + k_{13no} f_3 + \quad (1)$$
$$k_{12cc} f_1 f_2 + k_{13cc} f_1 f_3 + k_{41}T + k_{42}T^2$$

where the following notation has been used:

D = Dead zone

H = Histeresis

k_0 = bias, a new value for every use of the instrument,

k_{01} k_{02} = drift coefficients (modeling the linear and the quadratic variations with time t, respectively),

k_1, k_2, k_3 = coefficients of the polynomial approximation of the non-linear response characteristic to the specific force along the sensible input axis,

f_1, f_2, f_3 = specific forces, along the three input axes (denoted 1, 2 and 3),

k_{12no}, k_{13no} = coupling coefficients between the input axes, due to *n*on-*o*rthogonality,

k_{12cc}, k_{13cc} = cross - coupling coefficients,

k_{41}, k_{42} = coefficients of the polynomial dependence (linear and quadratic) of the sensor output signal from temperature T.

An equivalent equation to this one can be obtained for gyroscopes in which it is taken into consideration not its error model but an input/output approach, as if it were a black box. A result of a characterization of this kind can be seen in Faria et allii (2003), where no thermal characterization of the sensors has been performed.

It shall be noticed that the terms of the temperature compensation in the example of Equation 1 are of the second order. As previously mentioned, what is also true for the other terms, all the coefficients correspond to linear approximations of the behavior of the sensor around their points of operation. Nothing is more important than to keep the sensor in the vicinity of

its operating point, what can be obtained through the use of the system of the present work.

The objective of this work is to evaluate the reachable limits of precision of temperature control for miniature rate gyros under the variation of environmental conditions corresponding to Space applications.

Theoretical analysis is performed for the evaluation of the quality of the temperature control depending on parameters such as thermal resistances of mechanical interfaces; applied power dedicated for control; proportional, integral and differential gains. The analysis is based on thermal model of the assembly and direct simulation of the thermal behavior under various environmental conditions. The obtained results can be useful also for other inertial sensors.

2 Inertial Sensor assembly

Layout

For an inertial sensor designed for Space applications, its thermal conditions are defined through the conditions on its mechanical interface. Therefore, the stabilization of temperature can be carried out by providing a proper thermal control to the mechanical interface. Supplementary control can be applied to the sensor container in a tentative to compensate the variations of sensor internal heat dissipation. One of the possible configurations of such an assembly is shown in Figure 1. It consists of gyro case, mounted on satellite structural panel and fastened to it through the mechanical interface with the bolts having specific thermal resistance.
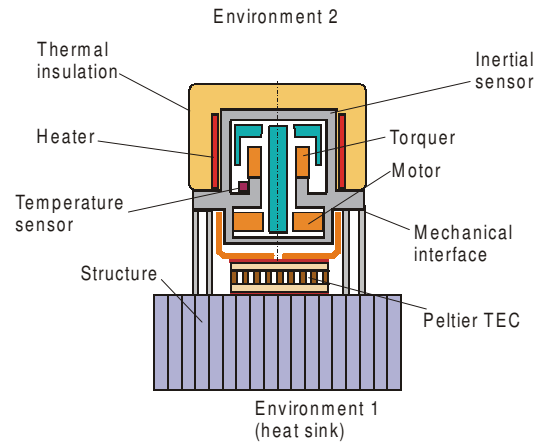

Figure 1. Layout of Gyro assembly mounted on structural panel.

The container is insulated from the upper environment by a layer of thermal insulation. The lower part of the gyro container, which is close to the mechanical interface, holds a good thermal contact with the Peltier thermal electric cooler (TEC) element. The opposite side of the TEC is

mounted on the internal face of the structural panel. The outer face of the panel, exposed to the outer heat sink environment, is used as a radiator to reject the heat dissipated by both the sensor and Peltier element. This heat sink environment, denoted as Environment 1 in Figure 1, is either outer Space for flight conditions, or airflow pumped with a fan for ground test conditions.

For ground testing the same configuration of the assembly above is used; the heat rejection is performed by either natural or forced convection (with a fan) from the outer (bottom) face of the panel. Usually Environment 1 and 2 (Figure 1) has the same ambient temperature for this laboratory conditions.

Thermal diagram

The equivalent thermal diagram of the assembly is shown in Figure 2. This diagram displays isothermal nodes and thermal couplings between them; heat sources and sinks are also shown.

The considered gyroscope is represented by nodes 1-7. Two internal elements are highlighted: torquer (node 2) and motor (node 3), because they produce heat dissipation $Q_{tq}(t)$ and $Q_M(t)$ [W] due to Joule's law heating.

Main distortion comes from outer Space (Environment 1) whose effective sink temperature varies in a very wide range.
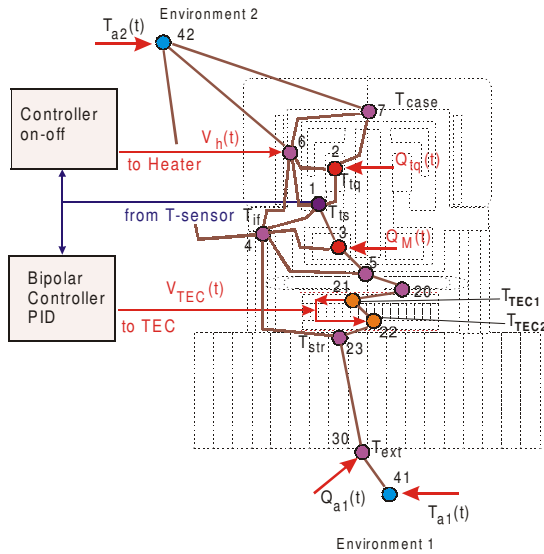

Figure 2. Thermal diagram

Control

The control heater and TEC of the assembly is tentatively performed by the on-off and PID type controller correspondingly.

The TEC is intended to compensate perturbations coming from the outer Space ambient (due to wide variation of incident fluxes from Sun, Albedo and Earth), whereas the heater is intended

to compensate perturbations because of variations in internal heat dissipation of motor and torquer.

For the TEC the controller must have bipolar DC current output feature to invert TEC action from cooling to heating (on upper junctions) if necessary.

Thermal mathematical model of the gyroscope

The thermal model is of the node type, representing the energy balance of each node, considering as isothermal. The transient energy balance can be expressed as

$$(Cm)_i \frac{dT_i}{dt} = Q_i(t) + Q_{ext,i}(t) +$$
$$\sum_j G_{i,j}(T_j - T_i) + \sum_j R_{i,j}(T_j^4 - T_i^4) \qquad (2)$$

Conductive couplings are defined through

$$G_{i,j} = \frac{k_{i,j} A_{i,j}}{L_{i,j}} \qquad (3)$$

Convective couplings are

$$G_{i,j} = h_{i,j} A_{i,j} \qquad (4)$$

Radiative couplings from the node i to outer Space can be expressed as

$$R_{i,j} = \sigma \varepsilon_i A_i \qquad (5)$$

Whereas inter-node radiative couplings must be calculated separately.

Where $k_{i,j}$ - effective thermal conductivity of a conductive path between nodes i and j [W/m/C];

$A_{i,j}$ - effective cross-section area of a path between nodes i and j [m^2];

$L_{i,j}$ - effective length of a path between nodes i and j [m];

$h_{i,j}$ - heat transfer coefficient between nodes i and j [W/C/m^2];

ε_i - emissivity of the surface of node i.

σ - Stefan-Boltzman constant. $5.67 \cdot 10^{-8}$ [W/K^4/m^2]

For ambient condition of laboratory testing the couplings for the nodes $i=6,7,4$ are

$$G_{i,42} = g_i A_i (T_{42} - T_i) \qquad (6)$$

and

$$G_{30,41} = h_{30} A_{30} (T_{42} - T_{30}) \qquad (7)$$

For Space conditions, for nodes $i=6,7,4$ $g_i=0$, $h_{30}=0$, and

$$R_{30,41} = \sigma \varepsilon_{30} A_{30} (T_{42} - T_{30}) \qquad (8)$$

and

$$Q_{ext,30}(t) =$$
$$\varepsilon_{30} A_{30} q_{IR}(t) + \alpha_{30} A_{30} (q_s(t) + q_a(t)) \qquad (9)$$

T_{42} - is effective Space temperature (2.9K)

Node 30 in Figure 2 represents the area of heat exchange to ambient; for Space condition it is a radiator with specified area A_r. Node 23 is the interface area of bond with one side of TEC element having an area of A_p. Thermal coupling between nodes 23 and 30 must include not only thermal resistance R_0 of panel, but also an additional thermal resistance of heat spreading For each i-th equipment the thermal conductance is defined as:

$$G_{23,30} = (R_0 + R_c)^{-1} \qquad (10)$$

Where

$$R_0 = \frac{\delta_p}{k_p A_p} \qquad (11)$$

$$R_c = \frac{\sqrt{A_r} - \sqrt{A_p}}{k_p \sqrt{\pi A_r A_p}} \times$$

$$\frac{\lambda k_p A_r R_0 + Tanh(\lambda \delta_p)}{1 + \lambda k_p A_r R_0 \cdot Tanh(\lambda \delta_p)} \qquad (12)$$

$$\lambda = \frac{\pi^{3/2}}{\sqrt{A_r}} + \frac{1}{\sqrt{A_p}}$$

Here δ_p and k_p are thickness and thermal conductivity of the panel. If a radiator panel provided for rejecting of heat to Space, when δ_p and k_p in the equation for R_c are properties of the radiator panel.

Model of TEC

Characterization of TEC

The main technical characteristics of TEC, usually presented by the manufacturers, are the following: Q_{max} (pumping heat, or maximal allowable dissipation on the TEC cold side [W]), ΔT_{max}, (maximal temperature difference [C]) V_{max} (maximal voltage, [V]) and I_{max}, (maximal electric current through TEC, [A]). All properties are given at specified hot-side temperature.

The basic equation for one of the TEC junctions is

$$Q = \mp nsIT + 0.5nI^2 R_{TEC} \pm nG_p \Delta T \qquad (13)$$

where n - is number of pellets; R_{TEC} - one pellet electrical resistance, [Ohm]; and G_p - one pellet thermal conductance, [W/K]; ΔT - temperature difference between junctions [C] (always >0 here). The main parameters are defined through specific parameters:

$$R_{TEC} = \rho(T) f_\delta, \quad G_p = k(T) \frac{1}{f_\delta}, \qquad (14)$$

$$f_\delta = \frac{\delta_p}{A_p}.$$

Here δ_p is the height of pellet [m], A_p - is the pellets cross-section area [m^2] and f_δ - is a form-factor.

The maximal temperature difference developed at the $Q_1=0$ conditions. Applying subscript 1 for cold junctions and 2 - for hot junctions, we have

$$0.5I_{max}^2 \rho(T_1) f_\delta^2 - s(T_1) I_{max} T_1 f_\delta + k(T_1) \Delta T_{max} = 0 \qquad (15)$$
$$T_1 = T_2 - \Delta T_{max}$$

Here T_2- is the specific hot-side temperature.

Equation (3) can be used to obtain first unknown parameter f_δ.

The product (nf_δ) can be found from the Ohm's law applied to the TEC at conditions when $Q_1=0$.

$$V_{max} = \frac{1}{2} n(\rho(T_1) + \rho(T_2)) f_\delta I_{max} \qquad (16)$$

Therefore, second unknown TEC parameters (n) can be obtained through the following relationships

$$T_1 = T_2 - \Delta T_{max}$$
$$(nf_\delta) = \frac{2V_{max}}{(\rho(T_1) + \rho(T_2)) I_{max}} \qquad (17)$$
$$n = \frac{(nf_\delta)}{f_\delta}$$

Consequently, the unknown parameter n and f_δ of TEC can be obtained through equations (15) and (17) with known T_2, Q_{max}, ΔT_{max}, V_{max} and I_{max} from technical supplier's specification of the selected cooler.

Transient TEC model

The principal operation of the TEC is characterized by junction temperatures T_{tec1} and T_{tec2}. The Peltier effect is expressed through electric current with its sign and the Seebeck coefficient. Thus it is like additional heat source and sink appear at the junction locations with corresponding heat consumption/dissipations

$$Q_{21}(t) = n\left(-s(T_{21}) I(t) T_{21} + 0.5I^2(t) \rho(T_{21}) f_\delta\right) \qquad (18)$$
$$Q_{22}(t) = n\left(s(T_{22}) I(t) T_{22} + 0.5I^2(t) \rho(T_{22}) f_\delta\right)$$

Here we accept that if the electric current is positive, 1st junction gets cooling, and the 2nd gets heating.

These two terms define the TEC function. The term I(t) [A] is the control action from the controller,

$$I(t) = \frac{2V(t)}{nf_\delta (\rho(T_{21}) + \rho(T_{22}))} \qquad (19)$$

The thermal coupling between two TEC junctions is defined as

$$G_{21,22} = \frac{n(k(T_{21}) + k(T_{22}))}{2f_\delta} \qquad (20)$$

Thermal capacitance terms are usual and are shown as components in the overall thermal model.

Control

The proportional-integral-differential (PID) type control is defined by the following equation for control function.

$$u = G_P\left((T_s - T_0) + G_D \frac{\bar{d}}{dt}(T_s - T_0) + \right. \tag{21}$$
$$\left. + G_I \int_{t-\Delta t_I}^{t} (T_s - T_0)dt \right)$$

The third term is executed during the integration period Δt_I. The second term is executed during the period of differentiation Δt_D

$$\frac{\bar{d}}{dt}(T_s - T_0) = \frac{1}{\Delta t_D} \int_{t-\Delta t_D}^{t} \left(\frac{dT_s}{dt} \right) dt \tag{22}$$

The control function is bounded by values ±1 for TEC and 0 to 1 - for heater. The output voltage of controller is therefore defined as

$$V(t) = u(t)V_{max} \tag{23}$$

The integral gain parameter, G_I, is sometimes known as the controller reset level. The effect of the integral term is to change the heater power until the time-averaged value of the temperature error is zero.

The on-off control is defined as

$$u = \begin{cases} 1, & \text{if } T_s < T_0 - \Delta T_0 \\ 0, & \text{if } T_s > T_0 + \Delta T_0 \end{cases} \tag{24}$$

The quality of the control will be evaluated through the analysis of temperature variation of the torquer, as most sensitive element of the gyroscope.

Results of modeling for ambient conditions

Case 1. No control; ambient temperature varies; no upper insulation on gyroscope; torquer dissipation is constant; interface legs are made from aluminum.

Amplitude of ambient temperature variation was set to 3^0C at average level of 25^0C; period of sinusoidal variation is 15 min.
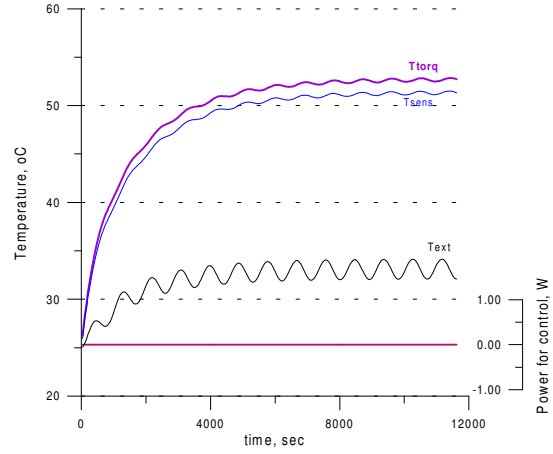
Figure 3. Temperatures of torquer (violet), T-sensor (blue) and external surface of panel (black).

Obtained results demonstrate that under variation of external ambient temperature of ±1.5 ^{0}C the torquer temperature varies from 50.95 to 51.44 ^{0}C (i.e. ±0.25 ^{0}C, amplitude is ΔT=0.5 ^{0}C) after quasi steady state settling. The reduction of temperature variations occurs due to thermal capacity of the IS. On account of such small variations of result temperature, there is no need of any thermal compensation.

Case 2. No control; ambient temperature is constant; torquer dissipation varies; no upper insulation on gyroscope; interface legs are made from aluminum.

The torquer dissipation was set to 1±0.5 W and period was varied from 10 sec. up to 5 min. The temperature variations for period of 2 min. are shown in Figure 4.
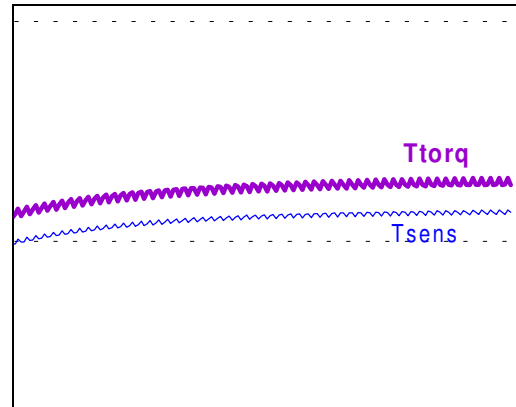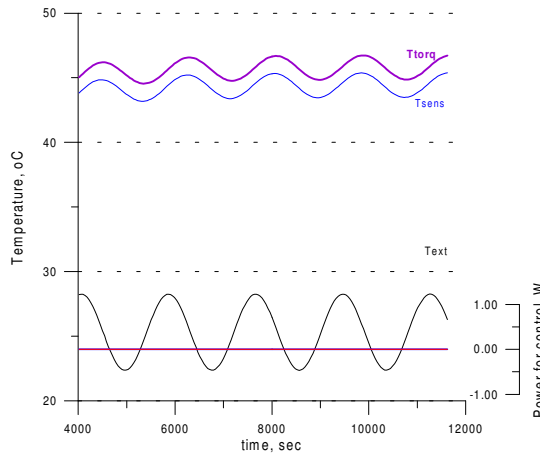

Figure 4. Temperatures of torquer and T-sensor, plotted versus time; scaled.

The results on torquer temperature variation are summarized below.

- Period is 10 sec: variation of temperature was not detected.
- Period 60 sec: temperature variation was found laying within the range of

52.56 to 52.75 ^{0}C (amplitude ΔT=0.19 ^{0}C)

- Period 2 min: temperature variation was found laying within the range of 52.55 to 52.89.^{0}C (ΔT=0.34 ^{0}C, see (Figure 4)
- Period 5 min: temperature variation was found laying within the range of 52.22 to 53.13 ^{0}C (amplitude ΔT=0.91 ^{0}C).

The values are figured out in the following table.

Period (τ) [sec]	T_{tq} [^{0}C]	ΔT_{tq} [^{0}C]
10	52.60	~0
60	52.56..52.75	0.19
2*60	52.55..52.89	0.34
5*60	52.22.. 53.13	0.91

The conclusion derived from simulation of this case is the following. In wide range of periods of oscillation from 10 sec to 5 min, the amplitude of the resulting oscillation of torquer temperature will not exceed 0.91 ^{0}C. These oscillations are small and it seems there is not a possibility and needas well to provide a control by thermal compensation.

Case 3. No control; ambient temperature varies, no upper insulation on IS; torquer dissipation is constant; interface legs are made from aluminum; fan cooling of the panel.

Figure 5. Temperatures of torquer (violet), T-sensor (blue) and external surface of panel (black).

The results of simulation on torquer temperature variation are summarized below.

- Period 10 min: temperature variation was found laying within the range of 45.5 to 46.1 ^{0}C (ΔT=0.6 ^{0}C)
- Period 20 min: temperature variation was found laying within the range of 45.15 to 46.45 ^{0}C (ΔT=1.3 ^{0}C)
- Period 30 min: temperature variation was found laying within the range of

44.86 to 46.73 ^{0}C (ΔT=1.9 ^{0}C, see Figure 5).

The obtained values are shown in the following table.

Period (τ) [sec]	T_{tq} [^{0}C]	ΔT_{tq} [^{0}C]
10*60	45.5..46.1	0.6
20*60	45.15..46.45	1.3
30*60	44.86..46.73	1.9

Therefore, compared to the case 1 where natural convection had been utilized for IS cooling, the application of fan cooling of the external surface of structural panel yields reduction on average temperature of torquer from about 51 ^{0}C to about 46 ^{0}C.

As for resulting variations of the torquer temperature, its amplitude was increased owing to better thermal coupling with varying ambient temperature. Maximal amplitude achieved is ΔT=1.9 ^{0}C, that generally could be compensated by switching-on the control features.

Case 4: Control with heater; ambient temperature varies; no upper insulation on IS; torquer dissipation is constant; interface legs are made from aluminum; fan cooling of the panel.

This case is derived from the case 2 for the period of ambient temperature variation set to 30 min (and amplitude of ΔT=3 ^{0}C). The amplitude of torquer temperature variation without control was 1.9 ^{0}C. For this case, on-off type of control is utilized with a heater as an actuator.
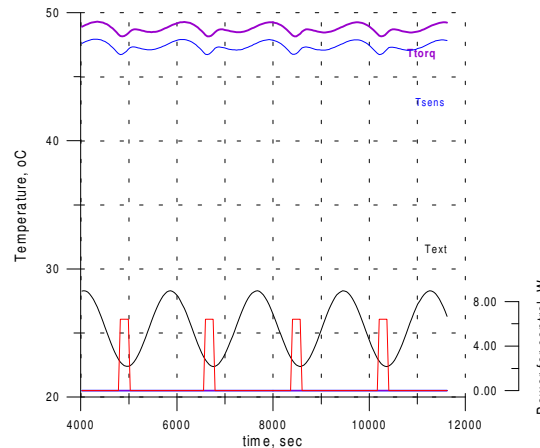

Figure 6. Temperatures of torquer (violet), T-sensor (blue) and external surface of panel (black); heat power consumed by controlled heater (red).

The maximal voltage directed to heater by a controller was set to 8 V, which corresponds to heating power of 6.4 W (on heater electrical resistance of 10 Ohm). Set point is 47 ^{0}C, and dead band is $\pm$ 0.2 ^{0}C.

The result of simulation shows that torquer temperature was varied from 48,15 to 49.25 ^{0}C (amplitude $\Delta T = 0.9$ ^{0}C).

If the maximum heater voltage will be accepted elevated, say 12 V, the control becomes worse, T= 48.24 to 50.29 ^{0}C ($\Delta T = 2.05$ ^{0}C). Thus, there exists an optimal value of the maximum heat power that can be directed to heater for precise control purpose.

Case 5: TEC PID control; ambient temperature varies; the IS is insulated; torquer dissipation is constant; interface legs are made from aluminum; fan cooling of the panel.

This case corresponds to conditions of the case 3. If no control is applied, the torquer temperature varies from 44.84 to .46.73 ^{0}C ($\Delta T = 1.9$ ^{0}C).

For this case, a Peltier thermo-electric element is activated for control features (and on-off control by heater is disabled). The parameters of the TEC element correspond ones for XLT2387 fabricated by MARLOW INDUSTRIES, Inc. (http://www.marlow.com): Q_{max}=21 W, ΔT_{max}=60 ^{0}C, V_{max}=3.7 V, I_{max}=8.9 A, T_{hot}=27 ^{0}C, A_1=25.4·10^{-3}x25.4.10^{-3} m^2, A_2=25.4·10-3x28.7·10^{-3} m^2.

The parameters of Proportional-Integral-Differential (PID) control have been set to the following values: T_{set}=50^{0}C, $V_{TEC} \le 1$V, proportional gain G_P=0.2 1/C, differential gain G_D=10 s and integral gain G_I=0.2 1/s. Integration and differentiation interval is 5 s.

The results of simulation are shown in Figure 7.
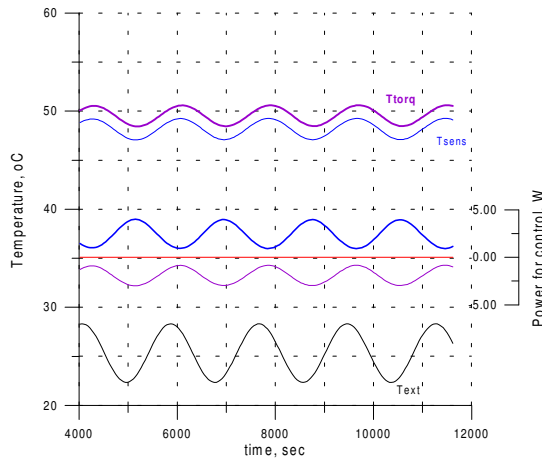
Figure 7. Temperature of torquer and T-sensor and heat flux developed by TEC, $V_{TEC} \le 1$V.

The result temperature variation of torquer obtained was within 48.57 to 50.61 ^{0}C, and amplitude is $\Delta T = 2.04$ ^{0}C, that is poorer than without any control (1.9 ^{0}C). From the Figure 7 it can be disclosed that the TEC works as a heater and does not present its reversible feature (i.e. heating-cooling). In an attempt to achieve this feature and improve the control quality, the increased limits of voltage supplied from the

controller to TEC (V_{TEC}) have been simulated. The results are the following.

$V_{TEC} \le 1.5$V, T_{tq}= 49.04 to 50.97 ^{0}C (amplitude $\Delta T = 1.93$ ^{0}C). Conclusion: there is still not enough electric power directed to TEC.

$V_{TEC} \le 2$V, T_{tq}= 49.47 to 51.09 ^{0}C (amplitude $\Delta T = 1.62$ ^{0}C). Conclusion: an improvement is clear, nevertheless there is still not enough electric power directed to TEC, otherwise set-point temperature does not selected correctly.
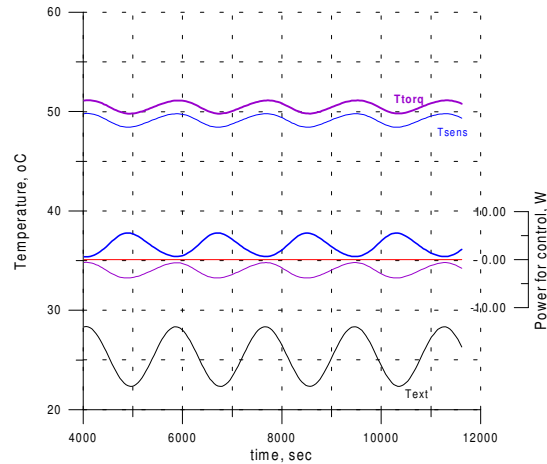

Figure 8. Temperature of torquer and T-sensor, and heat flux developed by TEC, $V_{TEC} \le 2$V

$V_{TEC} \le 2.5$V (note, V_{max}=3.7 V), result temperature is T_{tq}= 49.8 to 51.15 ^{0}C (amplitude $\Delta T = 1.45$ ^{0}C, see Figure 8). Conclusion is the same: a further improvement of control quality is clear, nevertheless there is still not enough electric power directed to TEC to achieve reversible feature, or the set-point temperature was not selected correctly. As a result, TEC continues to work as a heater.

Next we set the T_{set}, trying to obtain bi-polar TEC action. Such a set point was selected to T_{set}=45.0 ^{0}C. This resulted to reversible operation mode of the TEC, as it shown in Figure 9.
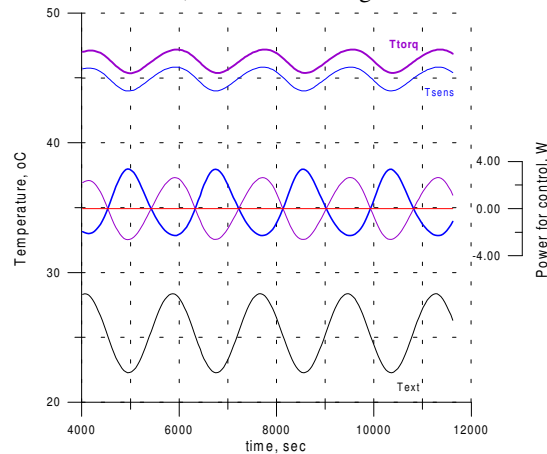

Figure 9. Bi-polar TEC action (heating-cooling)

The results of simulation confirm the variation of T_{tq} from 45.37 to .47.19 ^{0}C, with amplitude

ΔT=1.82 ^{0}C. PID parameters are: G_P=0.2C^{-1}, G_D=10 s G_I=0.2 1/s.

When a sensitivity analysis was performed in attempt to evaluate the influence of selection of the PID parameters to the temperature control quality. Results of this sensitivity analysis are summarized in the following table.

G_P [1/C]	G_D [s]	G_I [1/s]	ΔT [^{0}C]	T_{min} [^{0}C]	T_{max} [^{0}C]
0.2	10	0.2	1.82	45.37	47.19
0.1	10	0.2	2.29	45.07	47.36
0.4	10	0.2	4.59	44.66	49.25
0.2	5	0.2	1.84	45.36	47.2
0.2	20	0.2	1.77	45.4	47.17
0.2	10	0.1	1.84	45.36	47.2
0.2	10	0.4	1.76	45.39	47.15

The data shown were extracted at periods from 4000 s to 12000 s after establishment of quasi steady state regime, counted from the instant of powering up of the assembly. The obtained data demonstrate that to get a better control, gains G_D and G_I should be increased, whereas G_P is better to keep. Thus, if select G_P=0.2, G_D=30, G_I=0.6, the amplitude of torquer temperature variation gets further reduction, ΔT_{tq}=1.61 ^{0}C.

Below two graphs demonstrate entire transient processes from switching-on for two extreme variants of PID parameter selection: first, worst (G_P=0.4, G_D=10, G_I=0.2, Figure 10) and second, best (G_P=0.2, G_D=30, G_I=0.6, Figure 11).
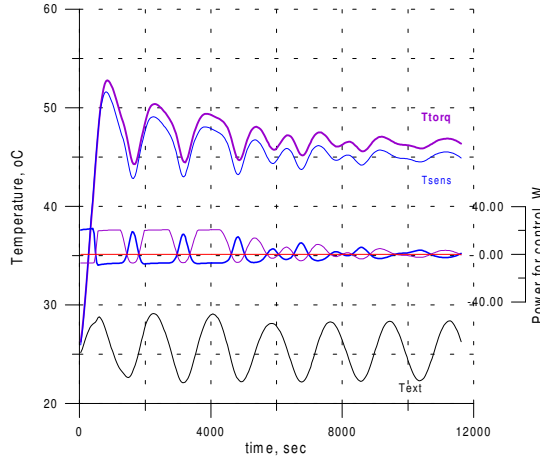
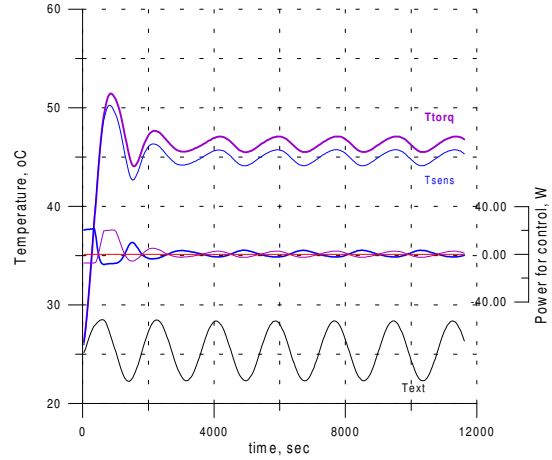
Figure 10. PID control under G_P=0.4, G_D=10, G_I=0.2

Figure 11. PID control under G_P=0.2, G_D=30, G_I=0.6.

As it is seen from the graphs, really, the second alternative (Figure 11) is better not only due to reduced amplitude of temperature variations after reaching quasi stedy state regime, but also because of much better dumping of initial over - shoot oscillations after switch-on.

Nevertheless, the control with heaters (Case 4) in general showed better results than PID control with TEC (Case 5) for ambient conditions: the lowest amplitude of temperature variation was 0.9 ^{0}C versus 1.61 ^{0}C.

Case 6: Obtaining low temperatures at ambient conditions by TEC, ambient temperature constant, the IS is insulated, torquer dissipation is constant, interface legs are made from aluminum or stainless steel; fan cooling of the panel .

The study of this case was performed to answer the question: how much the temperature of the IS assembly can be reduced by applying TEC for both purposes of cooling besides the control. The TEC is those of MARLOW INDUSTRIES, Inc. (XLT2387), which characteristics are given in description of Case 5.

The simulation was performed for alternative materials for IS mechanical interface legs: which is better, aluminum or stainless steel? Advanced fan cooling of structural panel (in Figure 2, this is environment 1, coupling 30-41), leading heat transfer coefficient increasing from 50 to 100 W/m^2/C, was also simulated. The results are summarized in the table posed below.

Upper limit of V_{TEC} [V]	$T_{tq,max}$ Al legs	$T_{tq,max}$ SS legs	$T_{tq,max}$ Al legs, advanced fan
0	45.81	79.52	45.74
1	41.05	54.67	40.95
1.5	41.02	48.59	40.9
2	42.33	45.91	42.17
2.5	44.83	46.05	44.63
3	48.39	48.49	48.14

| 3.5 | 52.85 | 52.81 | 52.53 |

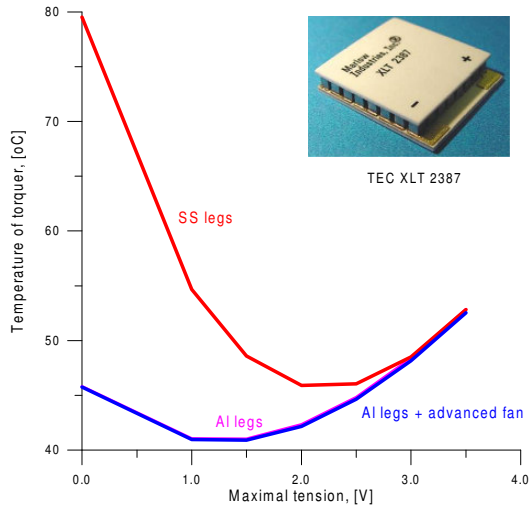The data from the table are plotted in Figure 12.

Figure 12. Temperature of torquer as function of tension supplied to TEC XLT2387

From the figure it can be seen that there is an optimal value of electrical tension supplied to TEC. Improving of fan cooling does not make sense. The enhanced thermal coupling between IS mechanical interface to structural panel (legs made from aluminum) present lower temperature of torquer. Anyway, minimal temperature obtained with such a TEC is about 41 ^{0}C. With stainless steel legs such a temperature is about 46 ^{0}C, in spite of considerable difference in thermal conductivity between aluminum and stainless steel (about one order of magnitude).

The last can be explained by the fact that principal heat output takes place through the Peltier element, so heat flux through interface legs does not cause significant change to final temperature.

To have an idea how the IS temperature could change if TEC were failed, a simulation was executed for the case of stainless steel legs. Transient temperature excursion is shown in Figure 13.
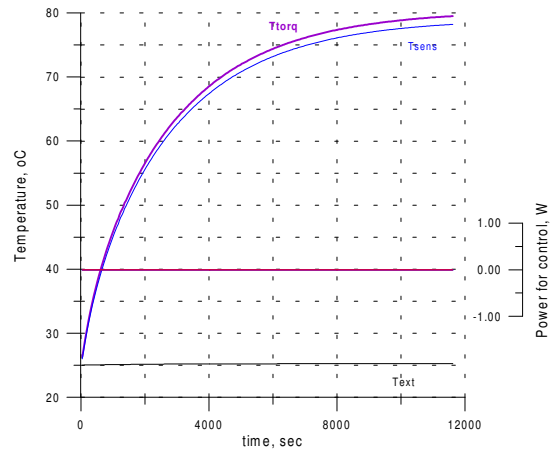
Figure 13. Temperature of IS torquer when TEC failed.

Note, how a long transient process could take place (more than 3 hours), and how much the temperature could be elevated (up to about 80 ^{0}C).

The transient process of heating up after switching on the IS assembly with TEC acting is shown in Figure 14 (tension is 1 V, aluminum legs).
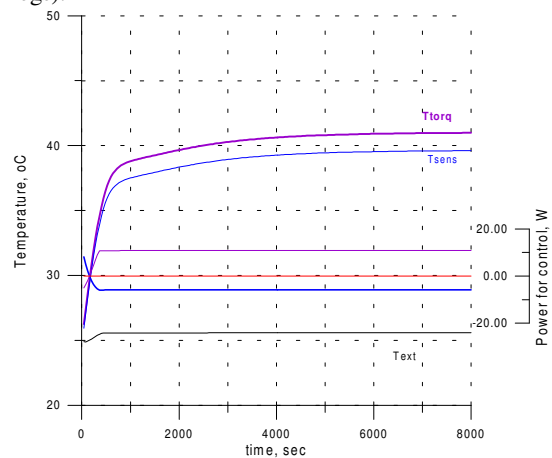

Figure 14. Typical transient with TEC action

For given conception, the minimum temperature achieved for ground test condition is about 41 ^{0}C. To reach lower temperatures, other configurations must be considered, additional study must be performed.

Case 7: Obtaining low temperatures at ambient conditions by different TECs, ambient temperature constant, IS is insulated, torquer dissipation is constant, interface legs are made from aluminum; fan cooling of the panel.

In this case we study how the proper selection of TEC element could affect the minimal reached temperature of the IS for ambient testing. We select among the coolers XLT2387, XLT2386 or XLT2385. Their parameters, derived from technical specification of the supplier, are given in the following table.

TEC	ΔT [°C]	Q_{max} [W]	I_{max} [A]	V_{max} [V]
XLT2385	56	127	13.9	14.1
XLT2386	56	72	13.9	8
XLT2387	60	21	8.9	3.7

The results of simulation are shown in the table posed below.

V_{TEC} [V]	T_{max} °C (XLT2387)	T_{max} °C (XLT2386)	T_{max} °C (XLT2385)
0	45.81	44.74	44.19
1	41.05	39.61	40.2
1.5	41.02	38.76	39.17
2	42.33	38.91	38.73
2.5	*44.83*	*39.96*	*38.83*
3	48.39	41.82	39.43
3.5	52.85	44.38	40.51
4		47.6	42.01
5		55.77	46.19
6		65.68	51.78
7		77.42	58.56
8			66.28
9			75.07
10			84.77

The data from the table are plotted in Figure 15.
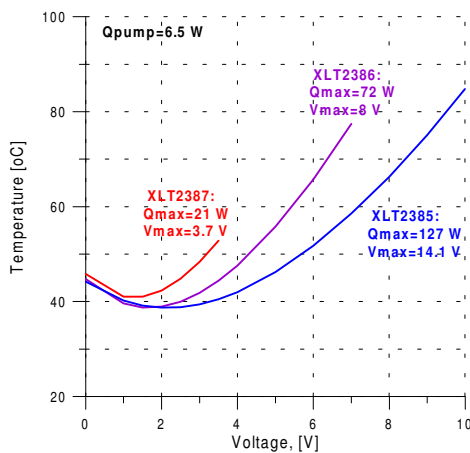
Figure 15. Temperature of torquer as function of input tension for different TECs

It is interesting to note, that for this particular case, the optimal value of input electrical tension varies within the range of 1.5 to 2.5 V whereas maximal permitted voltage varies from 3.7 to 14.1 V conforming to technical specification.

The transient process of heating up is shown in Figure 16 for the XLT2385, input tension is 2.5 V.
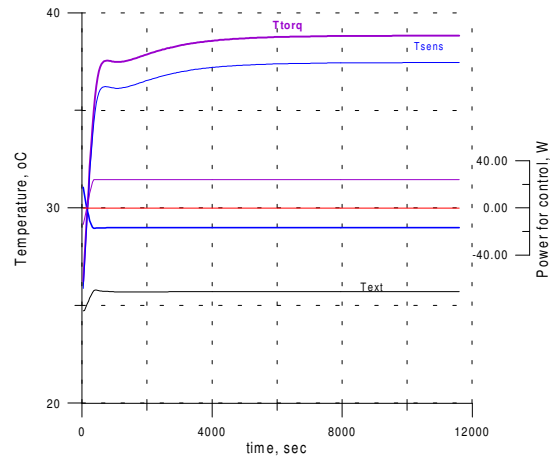
Figure 16. Heating up of IS with TEC PID control under ambient conditions.

In this study, the minimum temperature achieved by proper selection of TEC is about 39 ^{0}C. To reach lower temperatures, other configurations must be considered, additional study must be performed.

Results of modeling for Space conditions

Case 8: No control; interface legs are made from aluminum or stainless steel; painted area on honeycomb or radiator.

The Space conditions were simulated by enabling the external radiative heat transfer from external surface of the structural panel to outer Space with implied heat fluxes, which corresponds to the low-Earth orbit of about 750 km of altitude. It was assumed that infrared heat flux from Earth is constant, 59.2 W/m2, reflected flux (albedo) is absent and direct heat flux varies as shown in Figure 17.
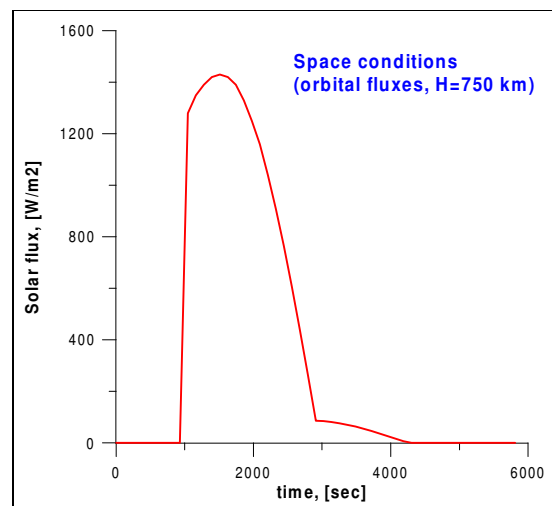

Figure 17. Implied direct heat flux from Sun

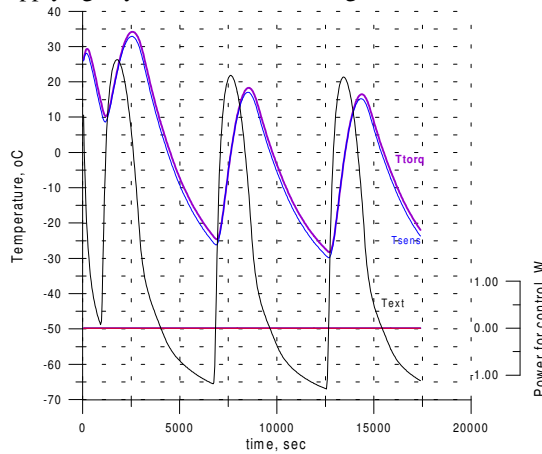The obtained temperature variations without applying any control are shown Figure 18.

Figure 18. Temperature variations during 3 orbits, no control, Al legs.

The result torquer temperature varies from -28.3 to 16.5 ^{0}C (amplitude ΔT=44.8 ^{0}C).

If the IS interface legs were made from stainless steel (poorer thermal coupling therefore), the torquer temperature would vary as shown in Figure 19.
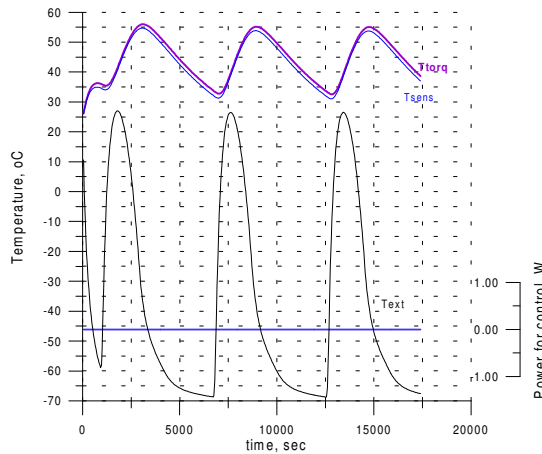

Figure 19. Temperature variations during 3 orbits, no control, SS legs.

The torquer temperature variation is from 32.54 to 55.16 ^{0}C (amplitude ΔT=22.6 ^{0}C).

From the last two figures it can be seen that in the condition of absent control, the partial thermal decoupling of IS mechanical interface from the structural panel allows reduction of amplitude of temperature variation from 44.8 down to 22.6 ^{0}C, whereas average temperature gets significant increasing from about -10 up to about +44 ^{0}C.

In an attempt to reduce the average temperature, a dedicated radiator, made of high thermal conductivity aluminum (thickness is 1.6 mm), can be attached to the external surface of the structural panel. The results of simulation for such a case are presented in Figure 20.
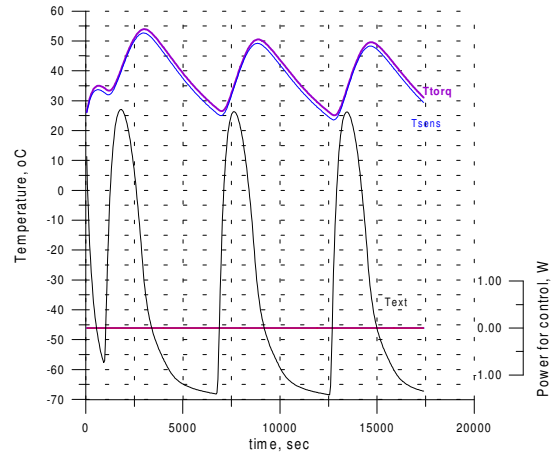

Figure 20. Temperature variations during 3 orbits, no control, SS legs, Al radiator.

The torquer temperature variation is similar to one previous case, from 25.1 to 50.51 ^{0}C (ΔT=25.4 ^{0}C). The average temperature decreases from 43.9 down to 37.8 ^{0}C.

Case 9: PID TEC control; interface legs are made from stainless steel; radiator.

The PID control by TEC XLT2387 is enabled. The PID parameters are taken optimized as the ones obtained from the sensitivity analysis conducted for Case 5 of the present paper. Input electrical tension is limited by $V_{TEC} \leq 1.5$ V, and the chosen set point temperature is 45 ^{0}C. The results of simulation are shown in Figure 21.
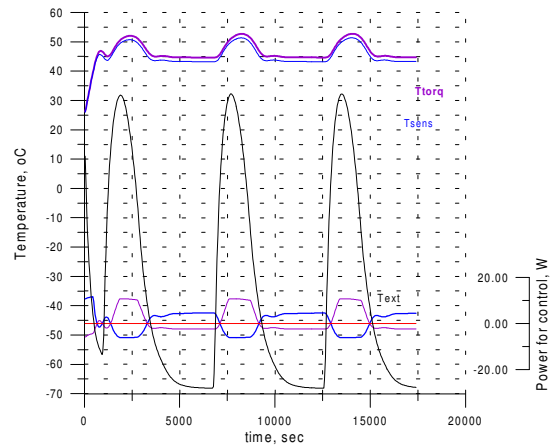

Figure 21. Temperature variations during 3 orbits, PID control of TEC, $V_{TEC} \leq 1.5$ V.

From the modeling, torquer temperature varies from 44.65 to 52.75 ^{0}C (ΔT=8.1 ^{0}C). The reversible feature of the TEC element is clearly seen form the figure: when panel is illuminated by Sun flux, the TEC acts as a cooler for IS; at eclipse the TEC acts as a heater. A time delay of reversing of TEC function (due to thermal capacity of the assembly together with the panel) can be also observed from Figure 21.

In an attempt to reduce the amplitude of temperature variation, the set point temperature was changed from ^{0}C. The results of simulation are shown in Figure 22.
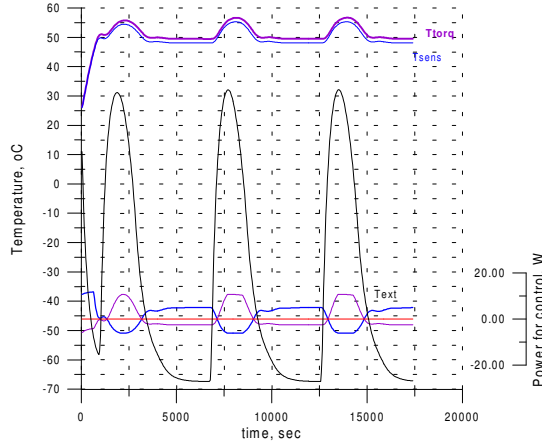

Figure 22. Temperature variations during 3 orbits, PID control of TEC, new set point.

The results confirm the variation of T_{tq} from 49.48 to 56.71 ^{0}C with amplitude of $\Delta T = 7.23$ ^{0}C

Next, the TEC was changed from XLT2387 to XLT2386 to check were a new Peltier element could present a better result. For input tension limited by $V_{TEC} \leq 1.5$ V, results are shown in Figure 23.
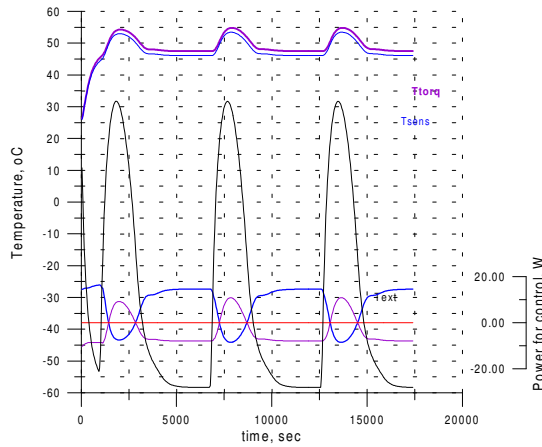
Figure 23. Figure 24. Temperature variations during 3 orbits, PID control of TEC XLT2386.

Next phase was to try to find optimal input tension. The results are summarized in the following table.

V<1.5 V, T=44.49..54.82 (dT=7.33 C)

V<2.0 V, T=48.43..54.19 (dT=5.76 C)

V<2.5 V. T=49.0 .. 53.72 (dT=4.72 C)

V<3.0 V. T=49.39..53.36 (dT=3.97 C)

V<4.0 V. T=49.88..52.88 (dT=3.00 C)

V<5.0 V. T=50.17..52.62 (dT=2.45 C)

Thus, the lowest amplitude of torquer temperature variation reached is 2.45 ^{0}C. Note, the optimal value of input tension (5V) is admirably different than one for cooling at ambient conditions (1.5 to 2.5 V). The best case of the control is illustrated in Figure 25.
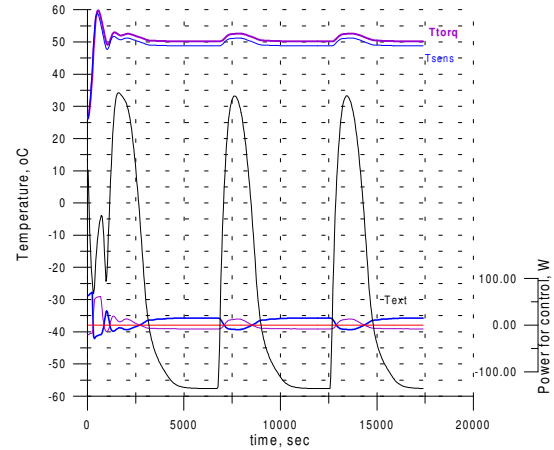

Figure 25. Temperature variations under TEC PID control with optimized parameters.

Further increasing of input tension does not make sense because the initial temperature overshoot becomes significant. Therefore, the best reachable precision of the IS temperature control for Space conditions, obtained during this study, is within of 3 ^{0}C range of torquer temperature variation.

Case10: Combined heater and TEC control; interface legs are made of stainless steel; radiator.

In this case we study if combined action of heater and TEC could provide finer control than TEC alone. First we try to enable heater with its on-off type of control and disable TEC. The set point temperature for the heater control was chosen $T_{set}=43$ ^{0}C and dead band is $\pm$ 0.5 ^{0}C. The results of simulation are shown in Figure 26.
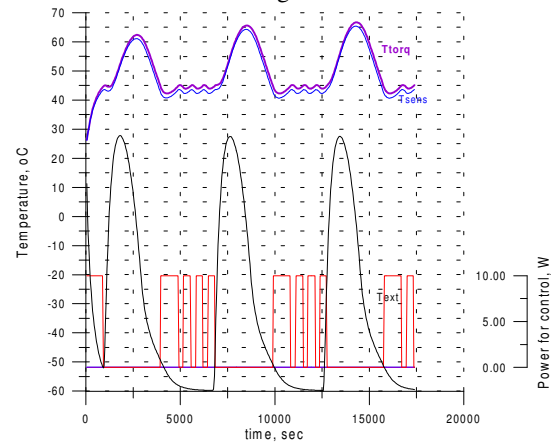

Figure 26. Control with heater alone.

Let us add the TEC with T_{set}=40 ^{0}C and V_{TEC}≤2V: The results of such a combined control are shown in Figure 27.
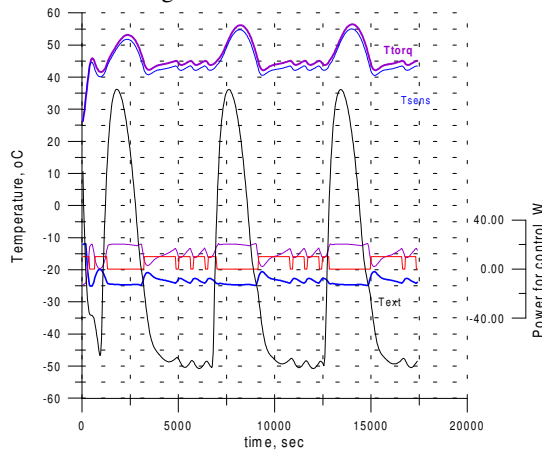

Figure 27. Combined action of heater and TEC.

In this graph, in the bottom section, red curve represents power consumption of heater; blue and violet curves represent heat consumption and generation on TEC opposite sides.

The obtained torquer temperature variations lie within the range from 42.13 to 56.43 ^{0}C (ΔT=14.3 ^{0}C). Note, that the maximum temperature was reduced compared to case of heater alone, due to the cooling action of the TEC.

Now we join set points of on-off and PID control, setting them to 43 ^{0}C. For input tension for TEC V_{TEC}≤2V we obtain the temperature variations, as shown in Figure 28.
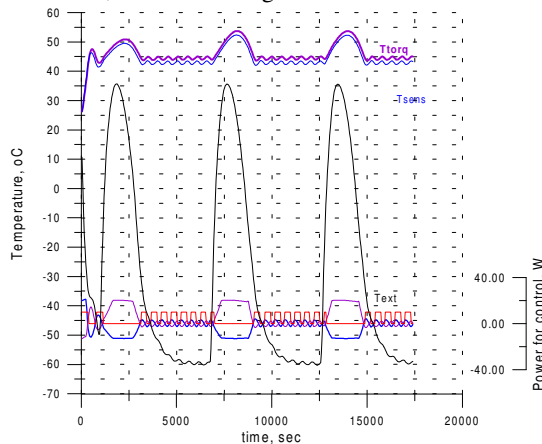

Figure 28. Combined action of heater and TEC for equal set points.

The resulting torquer temperature is T_{tq}=43.63 to 53.74 ^{0}C (ΔT=10.11 ^{0}C)

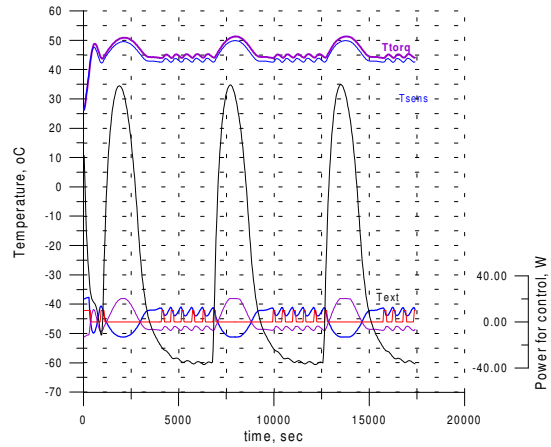Now we change T_{set} for TEC from 43 to 45 ^{0}C. Tthe results are presented in

Figure 29. Combined action of heater and TEC with different set points.

The results of modeling confirm the variation of T_{tq} from 43.95 to 51.28 ^{0}C with amplitude of ΔT=7.33 ^{0}C.

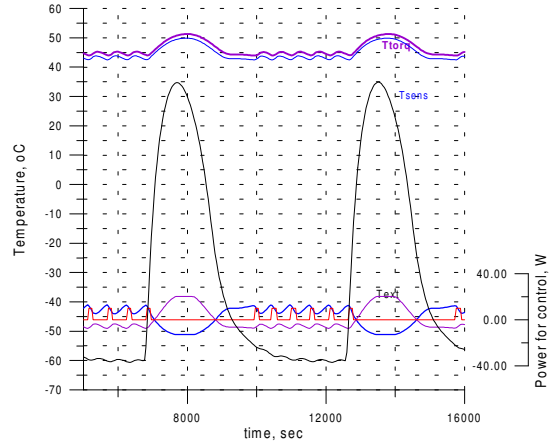In more details, interaction of combined controls is displayed in Figure 30.

Figure 30. Combined action during two orbits.

These preliminary results show that in order to achieve better precision of the combined control, further investigations are needed. Nevertheless, the following tendency in combined control can be already detected: The PID control with TEC presented better result than heater. Thus, gradually disabling of heater action, it is possible to come to TEC PID control alone, which already demonstrated precision of less than 3 ^{0}C of amplitude of temperature variations. It is partially confirmed from Figure 30, where it is seen that function of heater (red curve, in bottom section) is being partially taken by TEC (blue curve). Thus, it seems that the combined control does not provide benefits to the precision of thermal stabilization.

3 Conclusions

- If variation of dissipation of torquer has an average period less that ~2 min, this perturbation

can not be compensated owing to thermal capacity of the assembly: IS mounted on the base panel.

- Main perturbations come from the ambient of outer Space in flight configuration and not from internal variation of heat dissipation. It is not possible to insulated the IS from the Space ambient, because of the necessity to provide a path to heat rejection. Once this path is provided, the external thermal extremities will be transferred back to IS.

- Considering first two conclusions, the 3rd can be derived as the following: the installation of the internal temperature sensor does not make sense. For a heater the same is valid. External sensor and heaters are pretty enough.

- The best precision achieved for Space conditions for a given configuration of the assembly IS+TEC+heater is about 3^0 C of amplitude of temperature oscillation. The amplitude without control can reach the magnitude of 44^0 C. However, other possible orbits for a given mission should also be included in the analysis.

- For the given conception, the minimum temperature achieved for ground test condition is 39^0 C. To reach lower temperatures, other configurations must be considered, additional study must be performed.

- The selection of the right Peltier element (TEC) is not a trivial task. It can be performed only together with developing the complete thermal mathematical model. Particularly, the best TEC selected for this configuration has maximum transferring power of 71W on cold junction, that for first view could be considered as excessive, because the average power of IS here was 6.5 W. The reason is due to a high magnitude of coefficient of performance (COP) developed by TEC in such an operational mode.

- Combination of heater (on-off) and TEC (PID) for control does not make sense here, because the TEC in inverted mode produce enough dissipation to heat the IS.

4 References

Kondratiev, D. and Yershova, L. (2001). TE Coolers Computer Simulation: Incremental Upgrading of Rate Equations Approach. *Proceedings, Sixth European Workshop on Thermoelevtricity of the European Thermoelectric Society.* Freiburg im Breisgau, September 20-21, 2001. pp. 1-8

Faria, B.G.; Pereira, C.S.; Milani, P.G.; Santoro, C.A; Cunha S.P., Bueno, S.S.; Obtenção de parâmetros de aferição de uma unidade de medição inercial para aplicação em sistemas embarcados robóticos autônomos, *trabalho apresentado no VI Simpósio Brasileiro de Automação Inteligente.* Bauru, setembro de 2003.

R. Dorobantu, "Field Evaluation of a Low-Cost Strapdown IMU by means of GPS", *Ortung und Navigation,* DGON, Bonn, 1/1999.